

Effects of Blunting and Cooling on Separation of Laminar Supersonic Flow

J. DON GRAY* AND R. W. RHUDY†
 ARO Inc., Arnold Air Force Station, Tenn.

Experimental surface pressure and flowfield pressure survey measurements are presented and some comparisons with theory are made. As manifest by surface pressure data, the upstream extent of the viscous interaction induced on a flat plate by a 9.5° ramp was found to reach a maximum at an intermediate value of plate leading-edge radius as the radius was increased from 0.001 to 0.105 in. This effect was qualitatively unchanged by variations in freestream Mach number ($3 \leq M_\infty \leq 6$), flat plate Reynolds number ($0.25 \leq Re_c \times 10^{-6} \leq 1.0$), and wall temperature ratio ($0.1 \leq T_w/T_{t,\infty} \leq 0.9$). Comparisons of data for an adiabatic wall condition with calculations using a modification of the Lees-Reeves-Klineberg integral-moment theory show reasonable agreement and also indicate that the influence of Reynolds number may be significantly altered by leading-edge blunting for laminar flow reattachment. Wall cooling reduces the size of the ramp-induced viscous interaction region regardless of the location of transition relative to reattachment.

Nomenclature

M = Mach number
 p = static pressure, psia
 Re = Reynolds number based on freestream conditions and length, S
 R_N = nose radius, in.
 r = reattachment
 S = wetted axial distance from stagnation point, in. (see Fig. 1)
 s = separation
 T = temperature, $^\circ R$
 u/v = unit Reynolds number, in.^{-1}
 y = distance perpendicular to surface, in.

Subscripts

c = corner or hinge line
 FP = flat plate
 \bar{o} = value at beginning of interaction (see Fig. 5)
 t = total
 to = transition onset
 ∞ = freestream value
 w = wall

Introduction

IN the Mach number range $3 \leq M_\infty \leq 10$, a great number of experiments have been conducted with sharp-leading-edge ramp models at equilibrium wall temperature conditions. From these tests there has evolved a fairly clear picture of the influence of the important variables on the over-all interaction with a boundary layer which is initially laminar. In particular, the effects of model geometry, Reynolds number, Mach number, and transition upstream of but near to flow reattachment are all qualitatively well understood. Moreover the integral-moment theory developed by Lees, Reeves, and Klineberg¹ for laminar reattaching flow conditions predicts reasonably well the effects of Reynolds number, Mach number, and ramp angle on surface

pressure distributions. Very few investigations, however, have been concerned with conditions more representative of those experienced in flight. That is, the combined effects of leading-edge blunting and nonadiabatic wall temperature on the interaction between a laminar boundary layer and the inviscid flowfield have largely been ignored in the range $3 \leq M_\infty \leq 6$.

All of the experiments conducted to examine the effects of leading edge radius on ramp-induced laminar flow separation have been made at wall temperatures well below the adiabatic level. In addition, the only tests performed at $M_\infty \leq 6$ have been those of Holloway, Sterrett, and Creekmore,² who were concerned only with the effects on heat-transfer rate. The first investigation of leading-edge radius effects on surface pressure distributions was conducted by Townsend³ at $M_\infty = 10$ for a wall temperature ratio $T_w/T_{t,\infty} = 0.55$. Both of the above tests were concerned with laminar flow separations induced by short ramps deflected 10° or more. However, in both cases the flow reattachment was either 1) not free but instead was fixed by the limited ramp length at small deflections or 2) no longer laminar upstream of reattachment at large deflections. In tests conducted at $M_\infty \geq 14$ using a cold wall model without geometry limitations, Holden⁴ found that the influence of bluntness on the upstream extent of the interaction reached a maximum. That is, initially the interaction scale increased with an increase in leading-edge radius but then decreased for further increases in radius beyond an intermediate value of radius. This result was attributed to an interchange in the dominance of the local Reynolds number and Mach number as the leading-edge radius was varied. Thus, a better understanding of factors governing this interchange, particularly at supersonic Mach numbers, would be of considerable value in the design of control surfaces.

The present tests were conducted at nominal Mach numbers $M_\infty = 3, 4.5$, and 6 with plate Reynolds numbers $Re_c = 0.25, 0.5$, and 1.0 million. Longitudinal surface pressure and heat-transfer rates were measured at nominal temperature ratios $T_w/T_{t,\infty} = 0.9, 0.6$, and 0.3 at all Mach numbers. Additional measurements were made for $T_w/T_{t,\infty} = 0.1$ at $M_\infty = 6$. Boundary layer and flowfield pitot and static pressures were also measured on the flat plate and ramp at most test conditions.

Experimental Apparatus and Procedures

Wind Tunnels

The experiments were conducted in the von Kármán Gas Dynamics Facility (VKF), Supersonic Wind Tunnel (A), which

Presented as Paper 72-716 at the AIAA 5th Fluid and Plasma Dynamics Conference, Boston, Mass., June 26-28, 1972; submitted July 24, 1972; revision received March 2, 1973. This work was sponsored by the Air Force Flight Dynamics Laboratory (AFFDL), Flight Dynamics Control Criteria Division, Air Force Systems Command (AFSC), under Program Element 62201F, Project 8219.

Index categories: Supersonic and Hypersonic Flow; Jets, Wakes, and Viscid-Inviscid Flow Interactions.

* Group Supervisor, Projects Branch, Aerodynamics Division, von Kármán Gas Dynamics Facility. Member AIAA.

† Project Engineer, Projects Branch, Aerodynamics Division, von Kármán Gas Dynamics Facility.

has a flexible-plate nozzle and a 40- by 40-in. test section, and in the Hypersonic Wind Tunnel (B), which has an axisymmetric contoured nozzle and a 50-in.-diam test section. Both are continuous, closed-circuit, variable density wind tunnels. Tunnel A was operated at nominal Mach numbers of 3 and 4.5 at stilling chamber pressures from 9 to 37 psia and from 20 to 78 psia, respectively, and at a stilling chamber temperature of 600°R. Tunnel B was operated at a Mach number of 6 at stilling chamber pressures from 66 to 265 psia at a stilling chamber temperature of 850°R. The model was injected into the test sections for the data measurements and then was retracted for model cooling or model adjustments without interrupting the tunnel flow.

Model

The model (Fig. 1) consisted of 2.5-in. chord flat plate followed by a 9.5° ramp with a 5.0-in. chord. The flat plate aspect ratio (span/chord) was 10.4, a value sufficient to assure a large region of two-dimensional flow on either side of the centerline.⁵ Interchangeable leading-edge pieces were provided with radii $R_N = 0.001, 0.023, \text{ and } 0.105 \text{ in.}$

Internal cooling passages were provided in the model for the circulation of liquid nitrogen (LN_2) to lower the surface temperature.

Surface pressure taps (33) were distributed longitudinally within at least $\pm 0.25 \text{ in.}$ of the centerline, and wafer gages were mounted in the cylindrical support-transducer package just downstream of the model to minimize response time. Thermocouples (30) embedded near the surface were distributed over the entire model to verify the lateral and longitudinal uniformity of wall temperature. Eleven Gardon heat-transfer gages were located in a chordwise row, four on the flat plate, and seven on the ramp, 2.75 in. off the model centerline.

Pitot and static pressures in the flowfield were measured using a survey mechanism which was mounted to the model support and which was axially adjustable, as indicated in Fig. 1.

Procedures

For a cold wall test, the model was cooled to the desired wall temperature by circulating LN_2 through the internal passages and by spraying gaseous nitrogen over the surface to minimize frost accumulation. At the desired level, nitrogen flow was stopped, the transducer zeros were recorded, and the reference pressure for these transducers was established. The model system was then injected into the airflow, and after a delay of up to 10 sec the probe drive was initiated driving toward the surface. Monitor wall thermocouples indicated that the surface temperature was longitudinally and laterally uniform within $\pm 18^\circ\text{F}$ in the region of two-dimensional flow for most conditions during the time of data acquisition.

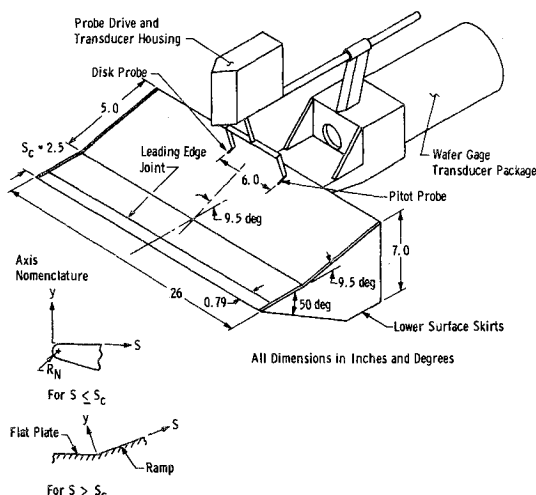


Fig. 1 Model dimensions.

Sym	S_c	Source
○	1.9	Unpublished Data
◊	2.5	Ref. 5
□	3.8	Unpublished Data and Ref. 8
△	7.6	Unpublished Data

Sym	M_∞	$(u/v)_\infty \times 10^{-6}$
Solid	3.0	0.05 to 0.20
Half Solid	4.5	0.03 to 0.25
Open	6.0	0.10 to 0.40

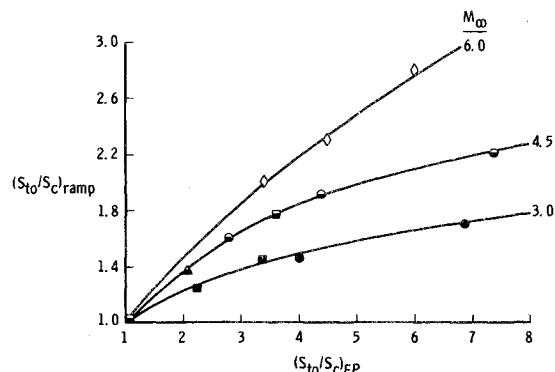


Fig. 2 Effect of Mach number on the relation between transition onset on a flat plate and a flat-plate-ramp combination ramp angle = 9.5° and $R_N \leq 0.001$ (adiabatic wall).

Flowfield static pressures were inferred from the disk probe measurements using the procedures outlined in Ref. 6 to correct for viscous interaction effects and probe misalignment.

The orifice dam technique⁷ was applied at selected conditions to define the approximate locations of separation and reattachment.

Results and Discussion

Onset of Boundary-Layer Transition

A correlation of the location of transition onset for the sharp-leading-edge model with an adiabatic wall is presented in Fig. 2 to illustrate the changes caused by the 9.5° ramp at the Mach numbers investigated. For example, knowing transition location on the flat plate at the freestream conditions of interest, it is obvious that $(S_{to}/S_c)_{FP}$ decreases as the distance to the hinge line, S_c , is increased and that this will, in turn cause the relative location of transition on the ramp, $(S_{to}/S_c)_{ramp}$, to move upstream toward reattachment. Thus, transition will be the farthest downstream of reattachment when S_c is as small as practical and laminar flow reattachment will be enhanced as much as possible. This figure also shows the considerable delay in transition onset resulting from an increase in freestream Mach number.

The effect of leading-edge blunting at $M_\infty = 6$ was shown by shadowgraph pictures to move transition onset downstream. In fact, at the highest Reynolds number tested, transition was not observed at all on the model when the blunted leading edges were

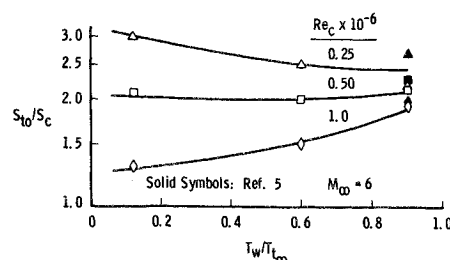
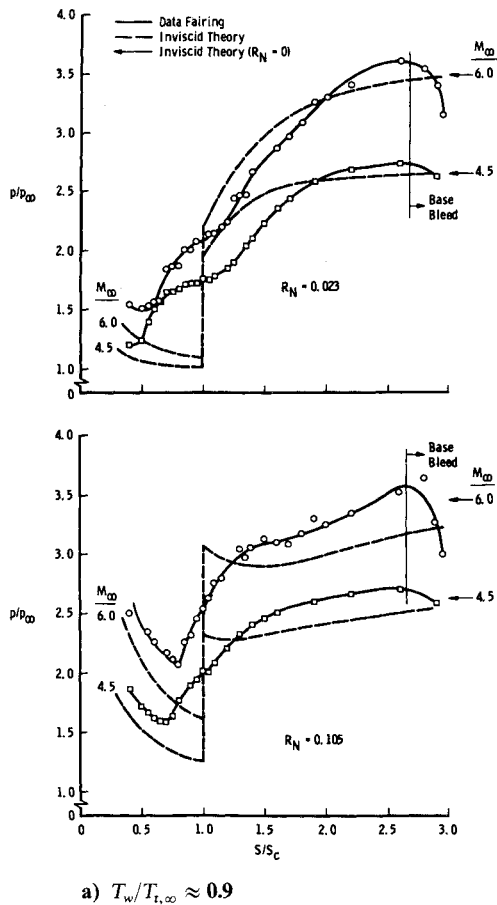
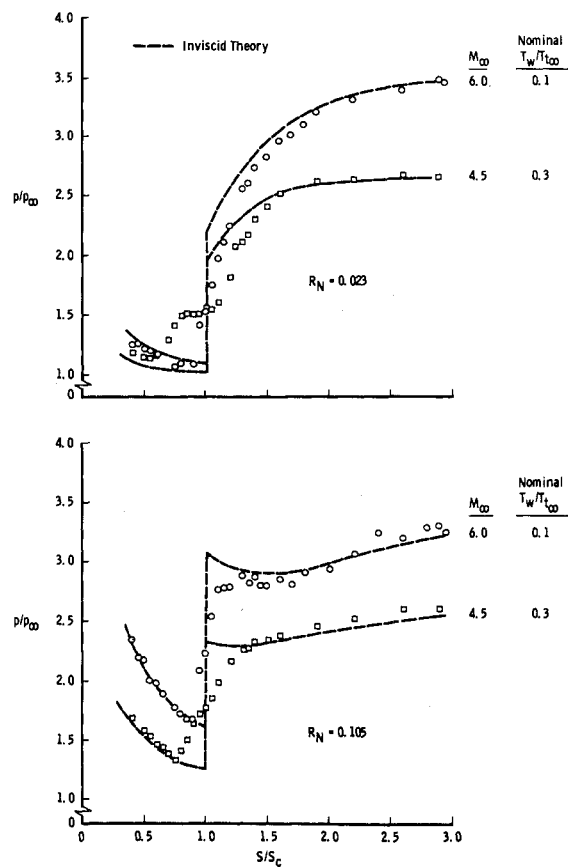


Fig. 3 Effects of Reynolds number and wall temperature on the relative transition location on a sharp leading-edge flat plate with a 9.5° ramp.

a) $T_w/T_{t,\infty} \approx 0.9$ 

b) Cold wall

Fig. 4 Comparison of inviscid and experimental surface pressure distributions on a 9.5° ramp model with blunt leading edges, $Re_c = 0.25 \times 10^6$.

installed.⁹ Since the results of Brinich and Sands¹⁰ indicate that transition onset on a flat plate is fairly independent of nose radius for the conditions of interest here, it is reasoned that at $M_\infty = 6$ nose blunting delayed transition primarily through its influence on the reattaching flow. Results of heat-transfer rate measurements on this ramp model⁹ indicate, however, that there was only a small effect of nose radius on transition at $M_\infty = 3$. Needless to say, the effects of bluntness on transition on flat plate or ramp configurations are not fully understood.

The effect of wall temperature ratio on transition onset was observable via shadowgraph pictures only at $M_\infty = 6$. These results indicated that the effect of blunting was essentially unchanged by cooling. However, it was found that the influence of wall temperature on transition onset for this ramp model was significantly affected by the value of plate Reynolds number. For example, Fig. 3 shows that transition moved upstream with wall cooling at $Re_c = 1$ million and that it moved downstream at $Re_c = 0.25$ million.

Effects on Surface Pressure Distributions

Theoretical inviscid pressure distributions (using the AMES/Lomax method of characteristics computer code) for $M_\infty = 4.5$ and 6 and $Re_c = 0.25$ million are compared in Fig. 4 with the blunted nose data for the adiabatic wall and cold wall temperature conditions. These inviscid results show that a substantial modification of the ramp pressure distribution is produced by a modest increase (0.023 in.) in leading-edge radius and that it is surprisingly similar to the viscous effects observed in the data for sharp leading edges.^{5,9} A significant discrepancy between inviscid theory and experiment is evident on the ramp in Fig. 4a at $S/S_c \gtrsim 2$, where it appears for $R_N = 0.105$ that the data have been shifted uniformly to higher pressure ratio. This effect was undoubtedly a result of the nearly isentropic compression in the hinge line region caused by the boundary-layer interaction. The oblique shock value for a sharp-leading-edge model, which is indicated by an arrow in Fig. 4a and which is not too far below the level of that for an isentropic compression at $M_\infty \leq 6$, is noted to be only slightly below the peak level for the data. However,

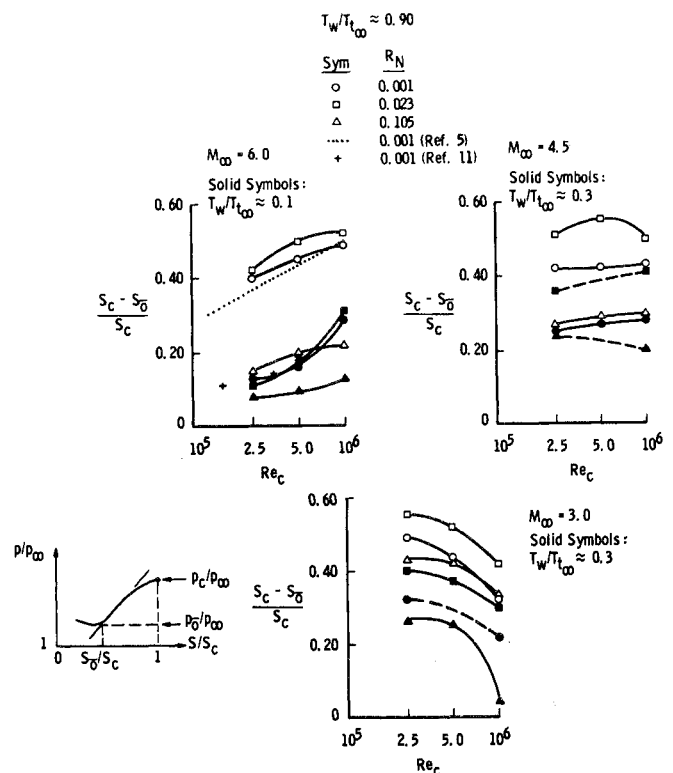


Fig. 5 Effects of plate Reynolds number on the upstream interaction extent.

with a cooled wall (Fig. 4b) inviscid theory and the data are remarkably close downstream of $S/S_c > 1.5$. This result is to be expected, since the boundary-layer interaction at the hinge line was drastically reduced by wall cooling and this caused the recompression to approach a finite, oblique shock wave in the limit of no interaction. Shadowgraph pictures show this change quite distinctly.⁹

Finally, it should be noted that the flat-plate results in Fig. 4 show that there were measurable and significant viscous interactions upstream of the ramp-induced interaction, even though the local Mach numbers at the boundary-layer edge were slightly less than 3.

Upstream Interaction Extent

A summary of the effects of plate Reynolds number variation on the relative extent of upstream interaction induced on the flat plate is shown in Fig. 5. Surface pressure data summarized in this form are useful for identifying the plate Reynolds number at which flow reattachment becomes transitional. That is, the extent of the interaction region increases with Reynolds number increase on sharp-leading-edge models as long as the flow reattachment remains laminar.⁵ Assuming that this criterion is also applicable to nonadiabatic wall and blunted-leading-edge cases, most of the $M_\infty = 3$ and some of the $M_\infty = 4.5$ data are indicated to have been transitional during reattachment.

The effects of leading-edge radius illustrated by the previous data are plotted in Fig. 6. In this form it is quite apparent that, with only one exception, the upstream extent of the interaction reached a maximum at an intermediate value of blunting and that this effect was generally observed regardless of the wall temperature ratio, freestream Mach number, or the likelihood of transitional flow reattachment. It is most likely that there was no flow separation at all R_N values for the one exceptional case at $M_\infty = 6$, $Re_c = 0.25$ million, and $T_w/T_{t,\infty} = 0.12$.

The effects of wall temperature ratio on the upstream interaction extent are shown in Fig. 7 for $Re_c = 0.25$ million. Wall temperature reduction with very few exceptions reduce the interaction scale not only at this Reynolds number but also at the maximum investigated.

Because the effects of Mach number on the interaction are so mixed, depending on the Reynolds number and wall temperature

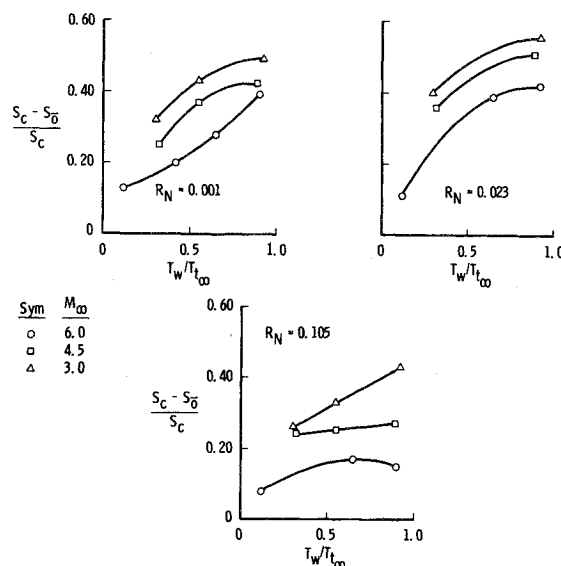


Fig. 7 Effects of wall temperature on the upstream interaction extent, $Re_c = 0.25 \times 10^6$.

ratio, no crossplots of the data are presented. The trend for a sharp-leading-edge model with laminar flow reattachment is to obtain a decreased interaction extent for a Mach number increase.⁵ This indeed was the case for the sharp leading edge at minimum

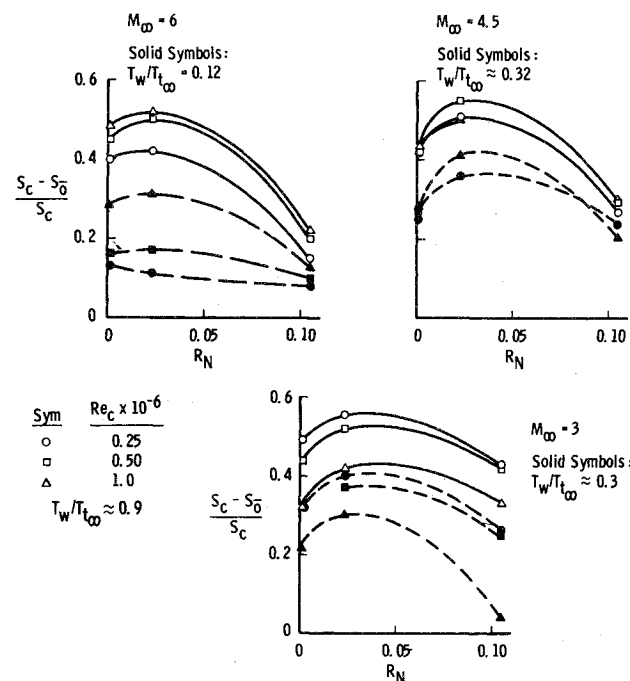


Fig. 6 Effects of nose radius on the upstream interaction extent for adiabatic and cold wall conditions.

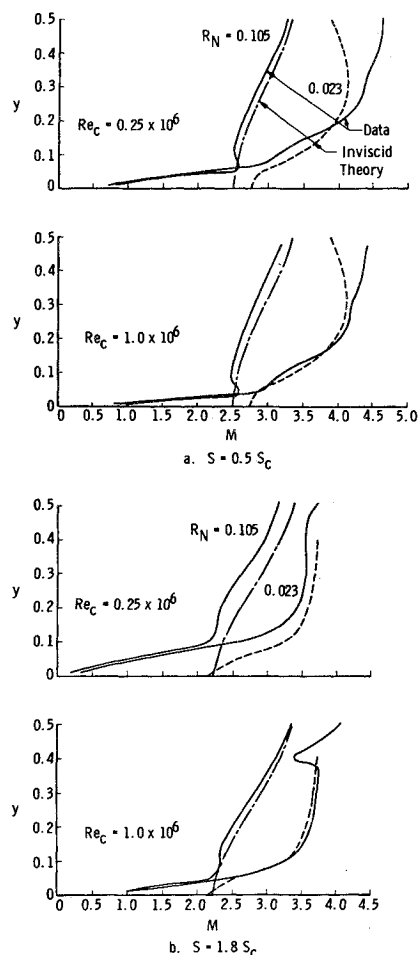


Fig. 8 Effects of nose radius on Mach number profiles on plate and ramp at $M_\infty = 4.5$.

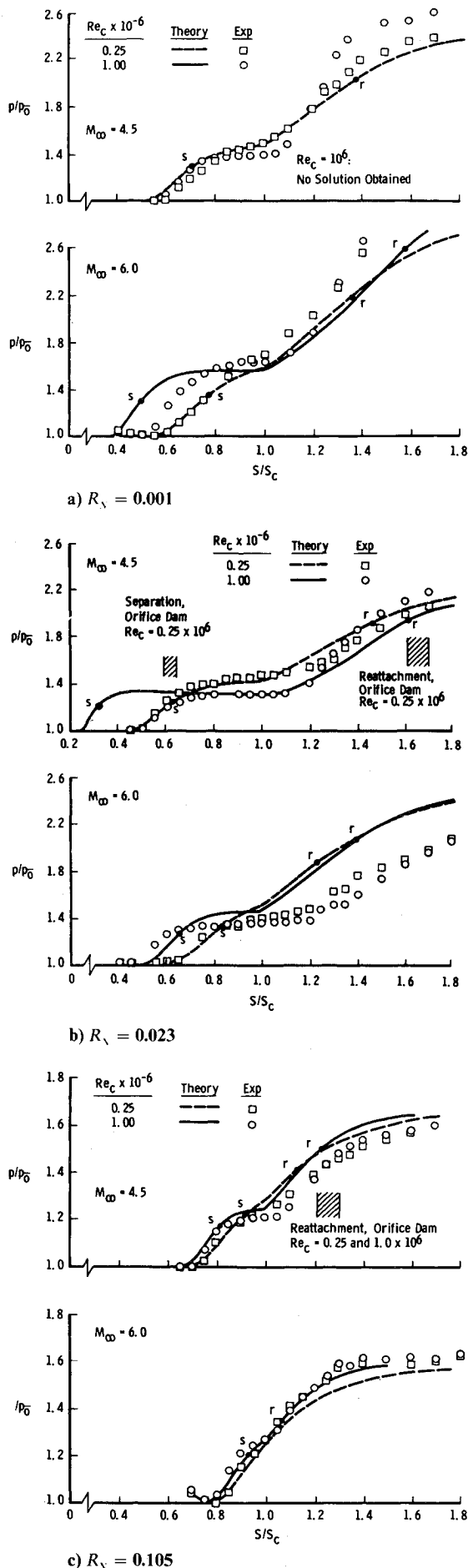


Fig. 9 Comparison of surface pressure data with modified integral-moment theory at low and high Reynolds number, adiabatic flow.

Reynolds number, as may be verified via the data in Fig. 5. Moreover, a similar trend was obtained more often than not with the blunt leading edges. The effect of Mach number is reversed at high Reynolds number because of the occurrence of transition prior to reattachment at low Mach numbers.

Flowfield Mach Number Profiles

Typical results from flowfield surveys made to determine the Rayleigh Mach number profiles are compared in Fig. 8 with inviscid Mach number profiles on the flat plate and ramp at $M_\infty = 4.5$ for the adiabatic wall case at the minimum and the maximum plate Reynolds number.

On the flat plate, surveys were made at a fixed station of $S = 0.5S_c$, which was well upstream of the beginning of the ramp-induced interaction for the bluntest nose ($R_N = 0.105$) but was at the approximate beginning for the intermediate nose ($R_N = 0.023$). These surveys are shown in Fig. 8a to be remarkably close to the inviscid profiles for $R_N = 0.105$ and reasonably representative for $R_N = 0.023$ in the entropy layers ($y \lesssim 0.2$). The discrepancy at $y > 0.2$ for $R_N = 0.023$ was primarily a result of poor agreement in the static pressure profile inferred by the disk probe measurements in this region. For the pitot pressure profiles, theory and data were in much closer agreement.⁹ Nevertheless, these results illustrate: 1) the significant reduction in local Mach number caused by leading-edge blunting and 2) the blending of the boundary layer ($y < 0.1$) into the entropy layer such that rather appreciable differences in Mach number at the boundary-layer edge may also result from plate Reynolds number changes.

On the ramp the surveys were made at $S = 1.8S_c$, a station which was well downstream of the expected reattachment position but which was somewhat upstream of the location indicated in Fig. 4 to be where the nominal inviscid level was reached when $R_N = 0.023$. These results are noted in Fig. 8b to be measurably different from the inviscid profiles for both nose radii at $Re_c = 0.25$ million, whereas they are in quite close agreement at the $Re_c = 1.0$ million. The data comparison at $Re_c = 0.25$ million suggests that the inviscid flowfield profile was displaced vertically (lifted) by the rather thick (about 0.1 in.) boundary layer. This, however, is not consistent with the similar comparison at $Re_c = 1.0$ million. Therefore, the apparent profile displacement at low Reynolds number for $R_N = 0.105$ is probably a result of the more isentropic compression process during reattachment, but for $R_N = 0.023$ it was caused by the proximity of reattachment to the survey station.

Comparisons with Integral-Moment Theory

Because of the significant effect of nose blunting on the plate and ramp inviscid conditions, the VKF developed computer code which utilizes the basic integral-moment theory of Lees, Reeves, and Klineberg¹ required modification to account for the changed boundary conditions. These modifications involved matching locally: 1) the inviscid pressure distribution on the plate and the inviscid ramp pressure at $S = 1.8S_c$, 2) the inviscid ramp Mach number at $S = 1.8S_c$, 3) the displacement thickness appropriate to the blunted plate at the location of the interaction onset, and 4) the estimated inviscid total pressure at the boundary-layer edge where the interaction begins.

Since the pressure calculated is usually nondimensionalized by the value calculated to exist at the interaction onset, the present calculations and data are also compared in this form vs the relative length. Results for the adiabatic wall condition only are presented in Fig. 9 to show the effects of nose radius, freestream Mach number, and plate Reynolds number.

The agreement of the data and calculations shown in Fig. 9a for the sharp-leading-edge configuration indicates that the flow reattachment was laminar for $M_\infty = 4.5$ and 6 at $Re_c = 0.25$ million. The degree of agreement between theory and experiment shown is typical of that usually found. At maximum Reynolds number, however, the data for $M_\infty = 4.5$ (certainly) and those at $M_\infty = 6$ (possibly) indicate transitional reattachment because of the lack of significant increase in the interaction relative to that at minimum Reynolds number. No solution was obtained for

$Re_c = 1.0$ million at $M_\infty = 4.5$ because convergence of the equations to establish the initial conditions for the integration could not be obtained. This occurs usually when the upstream extent gets too large (leading-edge separation approached) at low Mach number/high Reynolds number conditions.

Comparisons shown in Fig. 9b for the intermediate leading edge ($R_N = 0.023$) indicate the same evidence of transition effects at $M_\infty = 4.5$ (i.e., at $Re_c = 1.0$ million) and rather good agreement with the modified theory at $Re_c = 0.25$ million. Results obtained with ramp-type orifice dams to locate flow reversal at the low Reynolds number and $M_\infty = 4.5$ show very good agreement with the theoretical separation (s), whereas reattachment (r) is indicated to have been measurably downstream of the position calculated. Despite the very poor agreement shown on the ramp at $M_\infty = 6$, the agreement of theory and experiment upstream of the hinge line is surprisingly good. This discrepancy in ramp pressures indicates that the inviscid ramp Mach number specified for the solution should have been higher to account for the more isentropic compression in the presence of the viscous interaction.

Results for the bluntest leading edge tested ($R_N = 0.105$) are compared with calculations in Fig. 9c. The agreement is noted to be quite good, even though the comparisons with inviscid solutions (Fig. 4a) indicate significant reductions in the actual entropy rise during the ramp compression. Therefore, it is reasoned that compensating effects between the inviscid ramp pressure specified for a solution and the higher than inviscid total pressure on the ramp caused the inviscid ramp Mach number specified for the solution to be the appropriate value. These results strongly suggest that the lack of variation of the upstream interaction with a Reynolds number change was not necessarily caused by transitional flow reattachment. The orifice dam data at $M_\infty = 4.5$ are shown to agree with the calculated reattachment location rather well, and it is observed that the reattachment was moved upstream by the blunting increase.

These comparisons of theory with experiment generally confirm Holden's⁴ interpretation of data for much higher Mach number. That is, for small bluntness the effects of local Mach number decrease at the onset of the interaction override the opposing influence of local inviscid Reynolds number decrease there, but for larger bluntness the Reynolds number decrease at the boundary-layer edge becomes dominant and causes the interaction scale to shrink.

Summary

The tendency for transition to begin upstream of or near to flow reattachment increased as freestream Mach number decreased. For this reason, laminar flow reattachment at $M_\infty = 3$ was probably obtained only at the minimum plate Reynolds number. The effect of leading-edge radius increase on transition was to delay the onset at $M_\infty \geq 4.5$, primarily as a result of its influence on the reattaching flow.

The effect of wall cooling was to reduce the size of the ramp-induced viscous interaction regardless of the location of transition relative to reattachment. That is, this effect of wall cooling was

qualitatively unchanged by leading-edge radius, Mach number, or Reynolds number variations.

A small increase in leading-edge radius was found to have a greater effect on the over-all interaction studied than did a large increase. This effect was qualitatively the same regardless of the wall temperature ratio, freestream Mach number, or Reynolds number and is in general agreement with published data obtained at $M_\infty \geq 14$.

The integral-moment theory developed by Lees, Reeves, and Klineberg was modified to account for leading-edge blunting. Results calculated with this program are shown to agree reasonably well with the data for which the flow reattachment was laminar. In fact, such comparisons indicate that the variation of the upstream interaction extent with Reynolds number may be significantly modified by leading-edge blunting.

References

- ¹ Klineberg, J. M. and Lees, L., "Theory of Laminar Viscous-Inviscid Interactions in Supersonic Flow," *AIAA Journal*, Vol. 7, No. 12, Dec. 1969, pp. 2211-2221.
- ² Holloway, P. F., Sterrett, J. R., and Creekmore, H. S., "An Investigation of Heat Transfer within Regions of Separated Flow at a Mach Number of 6.0," TN D-3074, Nov. 1965, NASA.
- ³ Townsend, J. C., "Effects of Leading Edge Bluntness and Ramp Deflection Angle on Laminar Boundary-Layer Separation in Hypersonic Flow," TN D-3290, Feb. 1966, NASA.
- ⁴ Holden, M. S., "Leading-Edge Bluntness and Boundary-Layer Displacement Effects on Attached and Separated Laminar Boundary Layers in a Compression Corner," AIAA Paper 68-68, New York, 1968.
- ⁵ Gray, J. D. and Rhudy, R. W., "Investigation of Flat-Plate Aspect Ratio Effects on Ramp-Induced, Adiabatic, Boundary Layer Separation at Supersonic and Hypersonic Speeds," AEDC-TR-70-235 (AD719747), March 1971, Arnold Engineering Development Center, Arnold Air Force Station, Tenn.
- ⁶ Gray, J. D., "Evaluation of Probes for Measuring Static Pressure in Supersonic and Hypersonic Flows," AEDC-TR-71-265 (AD736017), Jan. 1972, Arnold Engineering Development Center, Arnold Air Force Station, Tenn.
- ⁷ Thomke, G. J. and Roshko, A., "Incipient Separation of a Turbulent Boundary Layer at High Reynolds Number in Two-Dimensional Flow over a Compression Corner," DAC 59819, Jan. 1969, Douglas Aircraft Corp., Santa Monica, Calif.
- ⁸ Gray, J. D., "Investigation of the Effect of Flare and Ramp Angle on the Upstream Influence of Laminar and Transitional Reattaching Flows from Mach 3 to 7," AEDC-TR-66-190 (AD645840), Jan. 1967, Arnold Engineering Development Center, Arnold Air Force Station, Tenn.
- ⁹ Gray, J. D. and Rhudy, R. W., "Effects of Wall Cooling and Leading-Edge Blunting on Ramp-Induced Laminar Flow Separation at Mach Numbers from 3 through 6," AEDC-TR-71-274 (AD738644), March 1972, Arnold Engineering Development Center, Arnold Air Force Station, Tenn.
- ¹⁰ Brinch, P. F. and Sands, N., "Effect of Bluntness on Transition for a Cone and a Hollow Cylinder at Mach 3.1," TN-3979, May 1957, NACA.
- ¹¹ Lewis, J. E., Kubota, T., and Lees, L., "Experimental Investigation of Supersonic Laminar, Two-Dimensional Boundary-Layer Separation in a Compression Corner with and without Cooling," *AIAA Journal*, Vol. 6, No. 1, Jan. 1968, pp. 7-14.